

## Dynamic Small-Angle X-ray Scattering System using an Imaging Plate

Shoji Suehiro,<sup>a</sup> Kenji Saijo,<sup>a</sup> Tetsuo Seto,<sup>a</sup> Naoki Sakamoto,<sup>a</sup> Takeji Hashimoto,<sup>a\*</sup> Kazuki Ito<sup>b</sup> and Yoshiyuki Amemiya<sup>c\*†</sup>

<sup>a</sup>Department of Polymer Chemistry, Graduate School of Engineering, Kyoto University, Kyoto 606-01, Japan, <sup>b</sup>Department of Synchrotron Radiation Science, Graduate University for Advanced Studies, Tsukuba 305, Japan, and <sup>c</sup>Photon Factory, National Laboratory for High Energy Physics, Tsukuba 305, Japan. E-mail: amemiya@kekvox.kek.jp

(Received 19 June 1995; accepted 15 May 1996)

A synchrotron-radiation dynamic small-angle X-ray scattering (SR-DSAXS) system using an imaging plate has been developed at the Photon Factory, National Laboratory for High Energy Physics, Japan, in collaboration with the Department of Polymer Chemistry, Kyoto University, Japan, for studying the dynamic response of mesoscopic structures in polymers to applied mechanical stimuli. Small-angle X-ray scattering patterns of  $100 \times 100 \text{ mm}^2$  have been successively recorded on a  $400 \times 200 \text{ mm}^2$  stage-mounted imaging plate with a minimum time interval of 0.5 s. X-ray data are simultaneously obtained with stress and strain measurements on specimens subjected to a mechanical deformation. The performance of the DSAXS system is demonstrated along with some experimental results concerning the dynamic deformation of a b.c.c. lattice with paracrystalline distortion in a co-polymer having spherical microdomains under a large oscillatory shear deformation.

**Keywords:** dynamic small-angle X-ray scattering; imaging plates; time-resolved measurements; shear deformation; colloids; polymers.

### 1. Introduction

Recent advances in the instrumentation of X-ray scattering, such as two-dimensional position-sensitive detectors (Lewis, 1994; Allinson, 1994) coupled with high-flux X-ray sources, such as synchrotron radiation, have made it possible to observe the deformation (Butler *et al.*, 1995) and the fracture processes (Ijichi *et al.*, 1993) of semicrystalline polymers in real time.

In the emerging field of 'soft materials', *in-situ* and time-resolved observations of X-ray or neutron scattering have been attracting increasing research interest in recent years. Among various soft materials, block co-polymer melts are of particular interest, showing a surprising variety of ordered patterns ('microdomain' structures) on a nanometer scale. The investigation of pattern formation in block co-polymers has become, in recent years, a fascinating research topic in the statistical mechanics of complex fluids. The ordered microdomain structures of block co-polymers are highly susceptible to external mechanical fields. The shear effects on the orientation and deformation of the spherical microdomain of block co-polymers have been investigated by several groups of researchers (Phoon, Higgins, Allegra, van Leeuwen & Staples, 1993; Koppi, Tirrell, Bates, Almdal & Mortensen, 1994; Okamoto, Saijo & Hashimoto, 1994).

*In-situ* time-resolved scattering experiments under shear are essential to understanding the structural mechanisms of shear deformation of block co-polymers and other mesostructured materials because their microscopic responses to applied stress can be observed. Simultaneous mechanical measurements and the observation of internal structures by time-resolved scattering or other optical methods using various types of radiation, such as X-rays, visible light or neutrons, during deformation of the sample is the basic concept of rheo-optics. In early studies on rheo-optics, the viscoelastic properties of semicrystalline polymers were investigated by the method of dynamic wide-angle X-ray diffraction (DWAXD) (*e.g.* Kawaguchi, Ito, Kawai, Keedy & Stein, 1968; Kawai, Nomura, Hashimoto, Suehiro & Fujita, 1988), which provides information on the time response of the crystalline phase. Dynamic small-angle X-ray scattering (DSAXS) (Suehiro *et al.*, 1988) is also one of the most promising methods of elucidating the relationship between the macroscopic properties and mesoscopic structures of a sample (Young, Kyu, Suehiro, Lin & Stein, 1983).

The present study is concerned with the development of a DSAXS system, which uses synchrotron radiation as a high-intensity X-ray source, an imaging-plate (IP) (Miyahara, Takahashi, Amemiya, Kamiya & Satow, 1986) system as a two-dimensional X-ray detector for time-resolved measurements, and a hydraulic driving system as a sample deformation device, in order to perform time-

† Present address: Department of Applied Physics, Graduate School of Engineering, University of Tokyo, Tokyo 113, Japan.

resolved measurements of changes in the structure of 'soft' ordered materials subjected to external fields.

As an X-ray area detector for time-resolved measurements, a stage-mounted imaging-plate system with an automatic stage controller was developed, replacing the formerly developed imaging-plate exchanger based on a cinema method (Amemiya, Kishimoto, Matsushita, Satou & Ando, 1989).

In this paper the design and construction of the DSAXS system are described. Some experimental results concerning the dynamic deformation of a body-centred cubic (b.c.c.) lattice in a block co-polymer having spherical microdomains under a large oscillatory shear deformation are presented in order to demonstrate the performance of the DSAXS system.

## 2. Instrumentation

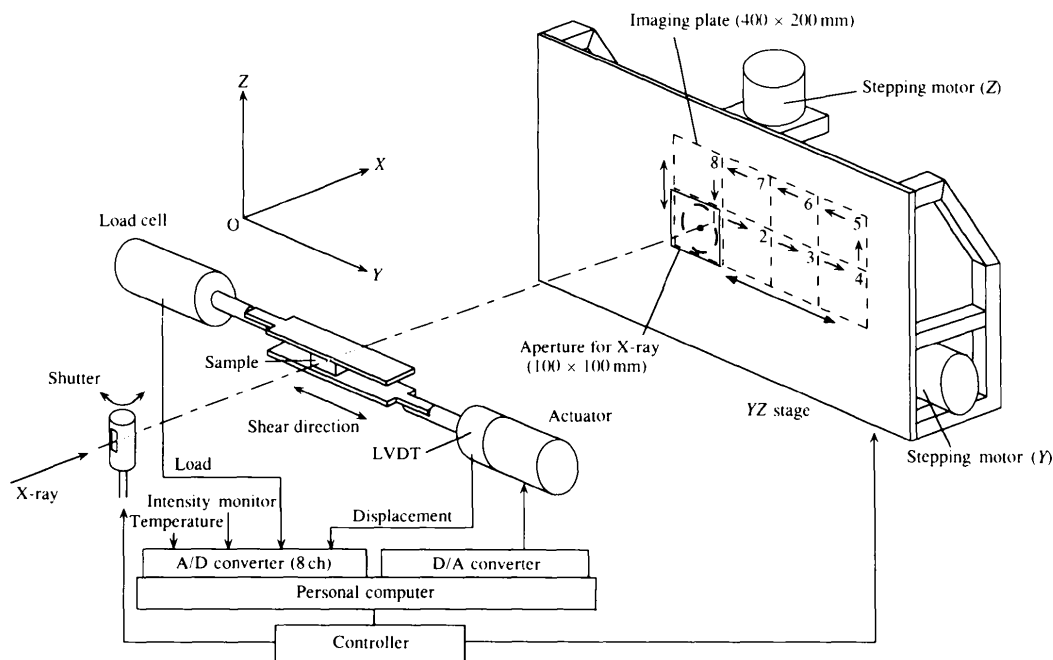
A synchrotron-radiation dynamic small-angle X-ray scattering (SR-DSAXS) system was constructed at beamline 15A of the Photon Factory, the National Laboratory for High Energy Physics, Japan. Beamline 15A has demagnifying mirror-monochromator optics (Amemiya *et al.*, 1983). The wavelength ( $\lambda$ ) of monochromatized X-rays was  $1.5 \text{ \AA}$  and its spectral distribution was  $\Delta\lambda/\lambda = 10^{-3}$ .

Fig. 1 shows a conceptual layout of the DSAXS system. The DSAXS system comprises a stage-mounted imaging-plate system developed at the Photon Factory and a hydraulic sample-deformation device developed at Kyoto University. Details concerning the sample-deformation device have been given elsewhere (Suehiro, Saijo, Ohta, Hashimoto & Kawai, 1986).

A sample can be uniaxially elongated or subjected to shear deformation. Fig. 1 shows the latter case. In either case the displacement of the actuator determines the macroscopic strain on the sample. The maximum load and maximum displacement are 490 N and  $\pm 7.5 \text{ mm}$ , respectively, and the operating frequency is between 0 and 60 Hz. The load on the sample is detected by a load cell, and the displacement of the actuator is measured using a linear variable differential transformer (LVDT). The temperature of the sample can be controlled at a constant value between 173 and 573 K by using a sample chamber made of a Cu block with heating elements and a channel of liquid nitrogen.

The Cartesian coordinate *OXYZ* is defined such that the *OY* axis is parallel to the deformation of the sample and the *OZ* axis is parallel to the shear gradient, or the vertical direction of the deformation device. The direction of the incident X-ray beam is along the *OX* axis in Fig. 1. However, it can also be aligned along the *OZ* axis by rotating the sample by  $90^\circ$  around the *OY* axis.

The imaging plate for time-resolved measurements is inserted into its cassette and is mounted on a *YZ* stage which is driven by two stepping motors through an intelligent stepping-motor controller. The *YZ* stage is made of two sets of conventional translation stages which are placed orthogonal to each other. In order to maximize the translation speed of the two stages, the weight of each stage is not loaded on the other stage. The load on each stage is just the weight of the imaging plate and its cassette. There is a  $100 \times 100 \text{ mm}^2$  square aperture for the scattered X-rays in front of the imaging-plate stage. An imaging plate ( $400 \times 200 \text{ mm}^2$ ) divided into eight sections ( $100 \times 100 \text{ mm}^2$ ) is used for



**Figure 1**

Schematic diagram of the DSAXS system consisting of a stage-mounted imaging-plate X-ray detector and a hydraulic sample-deformation device, both of which are controlled by a personal computer.

detecting SAXS patterns. Each section is moved to the position of the aperture in turn, as shown in Fig. 1, to record the X-ray pattern. The time required for the translational movement of the imaging-plate stage along the  $Y$  axis or the  $Z$  axis is *ca*  $0.5 \text{ s} (100 \text{ mm})^{-1}$ . Therefore, time-resolved measurements up to eight time slices are possible in a time scale shorter than  $1 \text{ s slice}^{-1}$ . The total number of frames for two-dimensional SAXS patterns per one imaging plate can be increased, and the dead time between successive measurements can be shortened accordingly by using a smaller aperture and a shorter sample-to-detector length at the expense of the spatial resolution of the X-ray scattering patterns.

The advantage of the present imaging-plate system for time-resolved measurements when compared with the previous one (Amemiya *et al.*, 1989) is that all of the successive X-ray patterns can be read out with only one scanning process with the standard imaging-plate scanner (BAS2000). In the previous system, since each time-resolved X-ray pattern was recorded on a separate imaging plate, the number of scanning processes required was as many as the number of the time slices.

A block diagram of the control system using a personal computer is shown in Fig. 2. The  $YZ$  stage on which an imaging plate is mounted [imaging-plate stage (1)] is driven by a pair of stepping motors. The stepping motors, which drive the  $Y$  and  $Z$  stages, respectively, are each controlled *via* an intelligent stepping motor controller (2)

by submitting command strings through an RS-232C serial communication line from a personal computer. Commands include setting the speed of each stepping motor in terms of pulses per second, movement to the mechanical origin of the imaging-plate stage, the relative movement in terms of pulses, and a request concerning the present position and status, which allow direct control of the  $YZ$  stage through the computer.

A solenoid-driven shutter (3) to shut off the incident X-rays is also controlled by the computer through an auxiliary digital output signal equipped within a digital-to-analogue (D/A) converter (4) board, which is mounted within the personal computer. The movements of the imaging-plate stage and the shutter are controlled in close connection with the phase angle of the cyclic strain applied to the sample.

The sample is deformed by a hydraulic actuator (5), which is controlled by a servo-controller such that either the load [from a load cell (6)] or displacement of the actuator [from an LVDT (7)] follows exactly the given reference signal, which is fed through a D/A converter (4). The D/A converter is operated by an interrupt handler, which is activated upon receiving a timer-interrupt signal; namely, a sequence of values of the reference signal written in computer memory in advance are read out by the interrupt handler and converted into an analogue signal by the D/A converter. This sequence is automatically triggered by a timing generator, which is also installed within the

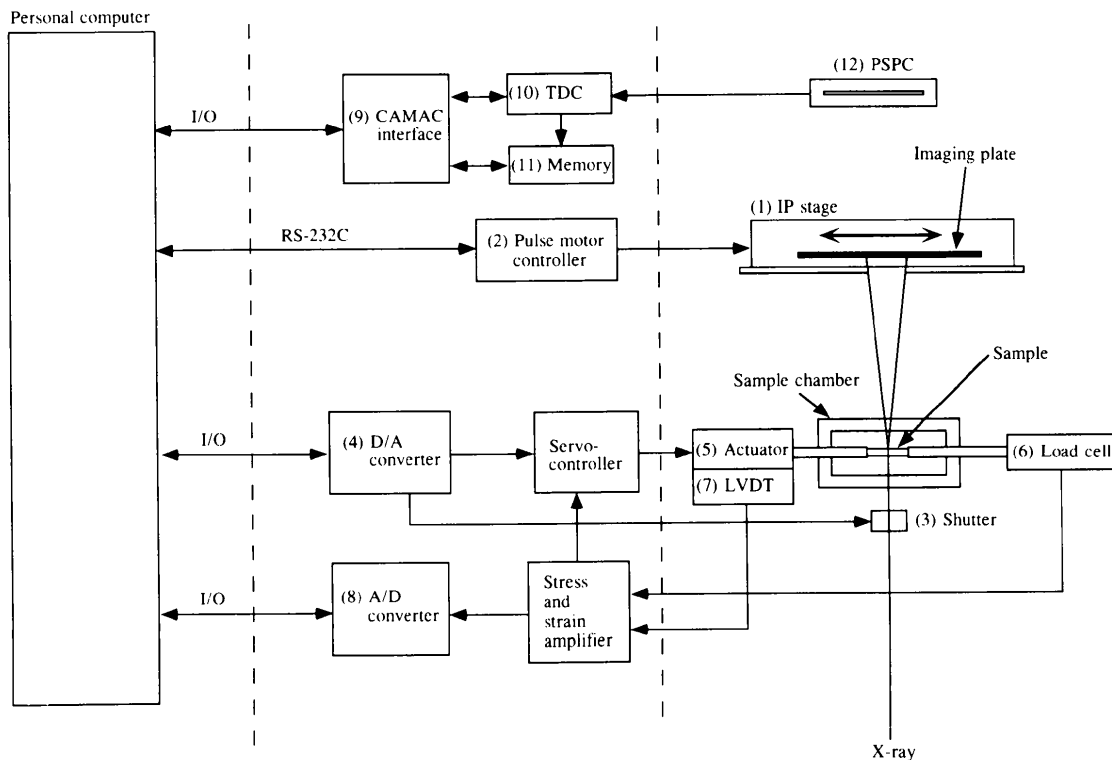


**Figure 2**

Block diagram of the control system for a synchronous recording of two-dimensional SAXS patterns with an applied dynamic deformation of the samples.

personal computer. The reference signal mentioned above determines the waveform of sample deformation, which is usually sinusoidal; the period of the timing pulse determines the frequency of the deformation.

The analogue data, such as stress and strain, can be sampled with an analogue-to-digital (A/D) converter (8) board, which is also installed within the computer, in synchronization with X-ray data acquisition performed by an imaging-plate system. This system also has a CAMAC interface (9), a time-to-digital converter (TDC) (10) and a histogram memory (11) in order to use a one-dimensional position-sensitive proportional counter (1D-PSPC) (12) as an alternative X-ray detector.

An example of a timing diagram is given in Fig. 3 in order to explain the DSAXS measurement. In this particular example, in the period designated as (1), the response of the two-dimensional SAXS pattern at a particular strain phase (e.g. strain maxima in the case of Fig. 3) is followed as a function of  $N$ , the number of strain cycles after the dynamic strain begins. In period (2), the dynamical response as a function of the strain phase is measured at a particular strain cycle. After cessation of the shear deformation at a particular strain level (e.g. at the maximum strain in the case of Fig. 3), relaxation of the system is observed during period (3). In order to carry out these various modes of data acquisition in a series of measurements, the control program has been designed to be driven by a set of parameter files in which detailed experimental conditions are defined.

### 3. Experiment

The sample studied is a polystyrene-*block*-poly(ethylene-*alt*-propylene) co-polymer [number-average molecular weight ( $M_n$ ) of  $3.4 \times 10^4$ , heterogeneity index ( $M_w/M_n$ ) of 1.3, where  $M_w$  is the weight-average molecular weight; the polystyrene (PS) volume fraction in the co-polymer is 0.103]. The co-polymer has spherical microdomains comprising polystyrene block chains in a matrix of poly(ethylene-*alt*-propylene) (PEP) block chains. The amplitude of the dynamic shear strain is 50%, the static strain is 0%, and the angular frequency is  $0.0944 \text{ rad s}^{-1}$ . Measurements were carried out at room temperature.

Previous studies (Okamoto *et al.*, 1994) show that the spheres are packed in a b.c.c. lattice with a paracrystalline

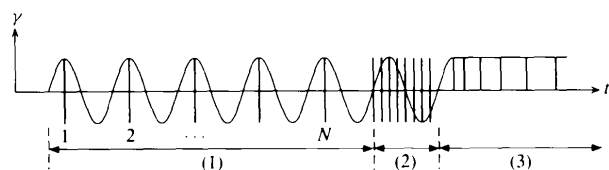
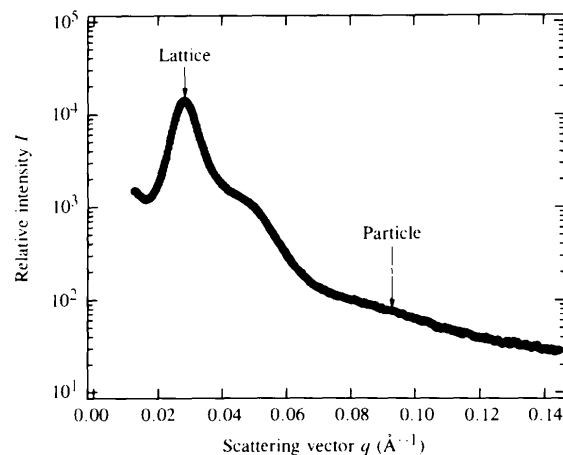


**Figure 3**

Example of a timing diagram of the DSAXS measurement. (1) Transient response as a function of the deformation cycle ( $N$ ). (2) Dynamic response as a function of the strain phase. (3) Transient response after cessation of the shear deformation.

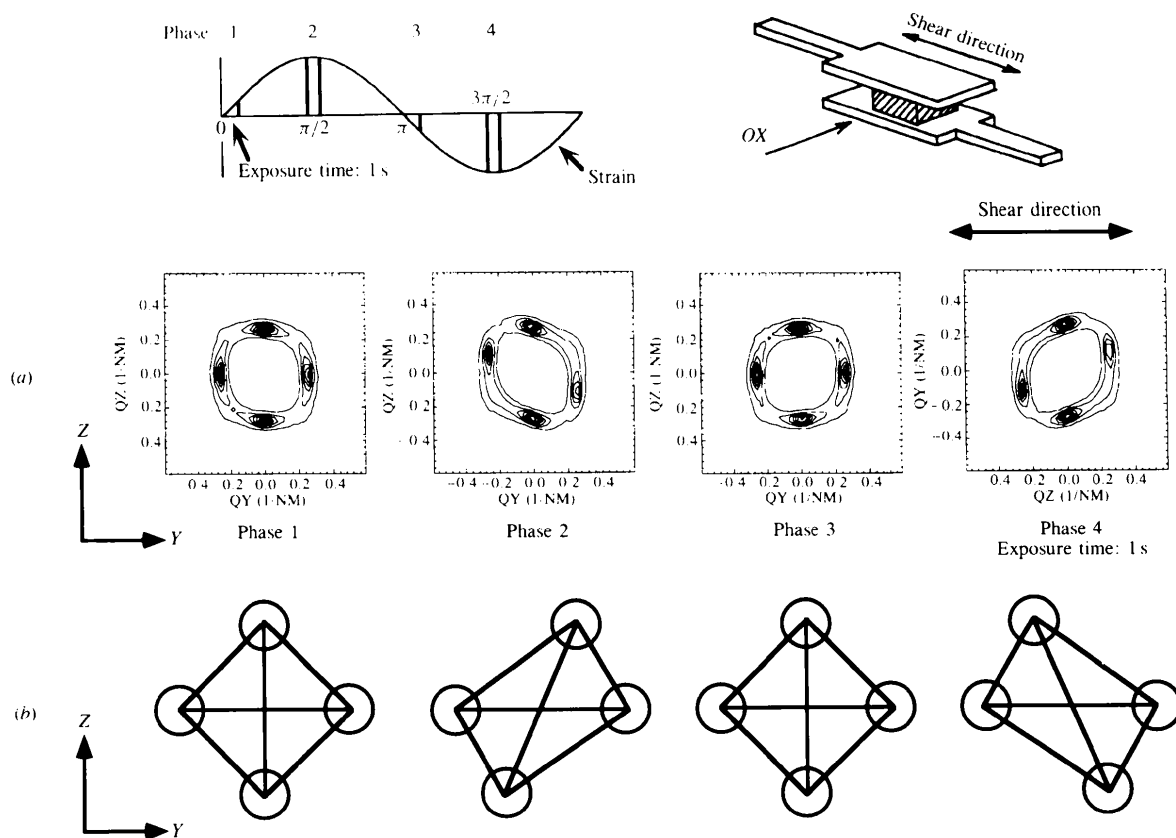
distortion of the second kind (Hosemann & Bagchi, 1962), and that the shear deformation induces a preferential orientation of (110) lattice planes parallel to the  $OXY$  plane. The two-dimensional SAXS pattern from an undeformed sample showed a circularly symmetric intensity distribution with respect to the incident beam axis, indicating that the b.c.c. lattice had a macroscopically random orientation. Fig. 4 shows the circular-averaged SAXS intensity distribution,  $I(q)$ , where  $q$  is the scattering vector defined by  $q = (4\pi/\lambda) \sin(\theta/2)$ ,  $\theta$  being the scattering angle.  $I(q)$  shows a sharp maximum at  $q_m = 0.0297 \text{ \AA}^{-1}$ , which corresponds to the Bragg spacing of the (110) lattice plane built up by the spherical microdomains of polystyrene. A broad maximum at  $q \cong 0.049 \text{ \AA}^{-1}$  consists of two scattering maxima superposed on each other due to the distortion of the second kind: the maxima are due to diffraction from the (200) and (211) planes, whose maximum positions are located at  $2^{1/2}$  and  $3^{1/2}$  relative to the first-order scattering maximum position, respectively. A paracrystal analysis (Matsuoka, Tanaka, Iizuka, Hashimoto & Ise, 1990) has shown that the  $g$ -factor characterizing the lattice distortion is  $0.09 \leq g \leq 0.13$ . A very broad maximum at  $q \cong 0.1 \text{ \AA}^{-1}$ , which can be more clearly discerned after subtracting the thermal diffuse scattering, reflects the form factor of single spheres; the number-averaged radius of the spheres was determined to be  $70.6 \pm 0.25 \text{ \AA}$  and the standard deviation from the mean radius ( $\sigma_R$ ) was found to be  $15.1 \pm 0.35 \text{ \AA}$  (Hashimoto, Kawamura, Harada & Tanaka, 1994).

Upon imposing an oscillatory shear deformation, the (110) and ( $\bar{1}10$ ) planes become oriented parallel and perpendicular to the  $OXY$  plane, respectively, resulting in a four-point SAXS pattern. The degree of orientation increases with the strain cycle ( $N$ ). Fig. 5 shows the SAXS patterns at four strain phases of  $0, \pi/2, \pi$  and  $3\pi/2$  ( $a$ ). These SAXS patterns were taken with an exposure time of 1 s for X-rays and at  $N = 110$  when the degree of (110) orientation reached the limiting value. Fig. 5 also shows a model



**Figure 4**

Circular-averaged SAXS intensity distribution profile for an undeformed sample of polystyrene-poly(ethylene-*alt*-propylene) block co-polymer.

**Figure 5**

SAXS patterns obtained at the four strain phases of shear strain (a) with a lattice-deformation model to explain the four diffraction spots of the (110) and ( $\bar{1}10$ ) planes (b). The X-ray exposure time was 1 s. The pattern at each strain phase was taken for a strain-phase interval of  $0.030\pi$  and at a strain cycle ( $N$ ) of 110.

used to describe the response of the lattice deformation at each strain phase, and to explain the four diffraction spots appearing in the two-dimensional SAXS patterns (b).

In response to the applied shear deformation, the b.c.c. lattice undergoes a dynamic lattice deformation. An interesting point is that in phases 1 and 3, where the magnitude of the shear strain is zero, the four-point patterns are almost identical, and both are symmetric with respect to both the  $OY$  and  $OX$  axes; also, the phase 2 pattern and the phase 4 pattern are mirror-images with respect to the  $OZ$  axis, indicating that the lattice deformation is approximately in-phase with the applied strain.

This observation is somewhat different from that of a previous study (Okamoto *et al.*, 1994) owing to the following two facts: (i) the previous result was obtained by cumulating the SAXS intensity over some period of the phase angle ( $0.384\pi$ ), whereas the present result was obtained over very narrow phase intervals ( $0.030\pi$ ); (ii) the previous result was obtained by cumulating the SAXS intensity at each phase interval over strain cycles from  $N = 80$  to 150, whereas the present result was obtained at a single strain cycle of  $N = 110$ . This may be a good example that the capability of the present SR-DSAXS system to carry out time-resolved SAXS measurements at shorter time scales gives better information concerning the deformation

mechanism of the internal structures at the mesoscopic level.

## References

- Allinson, N. M. (1994). *J. Synchrotron Rad.* **1**, 54–62.
- Amemiya, Y., Kishimoto, S., Matsushita, T., Satow, Y. & Ando, M. (1989). *Rev. Sci. Instrum.* **60**, 1552–1556.
- Amemiya, Y., Wakabayashi, K., Hamanaka, T., Wakabayashi, T., Matsushita, T. & Hashizume, H. (1983). *Nucl. Instrum. Methods*, **208**, 471–477.
- Butler, M. F., Donald, A. M., Bras, W., Mant, G. R., Derbyshire, G. E. & Ryan, A. J. (1995). *Macromolecules*, **28**, 6383–6393.
- Hashimoto, T., Kawamura, T., Harada, M. & Tanaka, H. (1994). *Macromolecules*, **27**, 3063–3072.
- Hosemann, R. & Bagchi, S. N. (1962). *Direct Analysis of Diffraction by Matter*. Amsterdam: North Holland.
- Ijichi, Y., Kojima, T., Suzuki, Y., Nishio, T., Kakugo, M. & Amemiya, Y. (1993). *Macromolecules*, **26**, 829–835.
- Kawaguchi, T., Ito, T., Kawai, H., Keedy, D. & Stein, R. S. (1968). *Macromolecules*, **1**, 126–133.
- Kawai, H., Nomura, S., Hashimoto, T., Suehiro, S. & Fujita, K. (1988). *High Modulus Polymers*, edited by A. E. Zachariades & R. S. Porter, pp. 363–429. New York: Marcel Dekker.
- Koppi, K. A., Tirrell, M., Bates, F. S., Almdal, K. & Mortensen, K. (1994). *J. Rheol.* **38**, 999–1027.
- Lewis, R. (1994). *J. Synchrotron Rad.* **1**, 43–53.
- Matsuoka, H., Tanaka, H., Iizuka, N., Hashimoto, T. & Ise, N. (1990). *Phys. Rev. B*, **41**, 3854–3856.

- Miyahara, J., Takahashi, K., Amemiya, Y., Kamiya, N. & Satow, Y. (1986). *Nucl. Instrum. Methods*, **A246**, 572–578.
- Okamoto, S., Saijo, K. & Hashimoto, T. (1994). *Macromolecules*, **27**, 3753–3758.
- Phoon, C. L., Higgins, J. S., Allegra, G., van Leeuwen, P. & Staples, E. (1993). *Proc. R. Soc. London Ser. A*, **442**, 221–230.
- Suehiro, S., Hendricks, R. W., Lin, J. S., Kyu, T., Young, P. & Stein, R. S. (1988). *J. Polym. Sci. Polym. Phys. Ed.* **26**, 745–770.
- Suehiro, S., Saijo, K., Ohta, Y., Hashimoto, T. & Kawai, H. (1986). *Anal. Chim. Acta*, **189**, 41–56.
- Young, P., Kyu, T., Suehiro, S., Lin, J. S. & Stein, R. S. (1983). *J. Polym. Sci. Polym. Phys. Ed.* **21**, 881–892.